THE ASTROPHYSICAL JOURNAL, 382:544–554, 1991 December 1

ASYMPTOTIC THEORY FOR THE SPATIAL DISTRIBUTION OF PROTOSTELLAR EMISSION

FRED C. ADAMS
Harvard-Smithsonian Center for Astrophysics, 60 Garden Street, Cambridge, MA 02138
Received 1991 March 14; accepted 1991 May 21

ABSTRACT

In order to facilitate the interpretation of observations of protostellar sources, we develop an analytic theory of protostellar emission. We focus our discussion on submillimeter wavelengths where protostellar sources can be spatially resolved. For a given protostellar envelope (i.e., given density and temperature distributions), we determine an asymptotic expansion for the specific intensity. We then calculate the convolution of specific intensity profiles with the Gaussian response function of a telescope. Using these analytic results, we calculate the monochromatic luminosity ratio $L_\nu(R)/L_\nu(0)$—a directly observable quantity—in terms of the underlying physical quantities. Observations of $L_\nu(R)/L_\nu(0)$ can be used in conjunction with the results of this paper to estimate the physical parameters of protostellar envelopes (in particular, the effective power-law indices p and q of the density and temperature distributions).

Subject headings: spectrophotometry — stars: evolution — stars: formation — stars: pre–main-sequence

1. INTRODUCTION

Our understanding of the star formation process is rapidly growing. Although the identification of actual protostars (forming stars which are actively gaining mass from the interstellar medium) has been elusive (see, e.g., Wynn-Williams 1982), many protostellar candidates have now been discovered and studied over the last decade (see, e.g., Beichman et al. 1986; Myers et al. 1987; Beichman 1987; Ladd et al. 1991a). The spectral energy distributions of many of these objects are in good agreement with spectra calculated from the current protostellar theory (see the review of Shu, Adams, & Lizano 1987; Adams, Lada, & Shu 1987). These results suggest that protostellar objects are composed of a central star/disk system which is deeply embedded within an infalling envelope of dust and gas. The spectral signature of protostars is largely determined by the properties of the protostellar envelope which absorbs and reradiates most of the energy from the central star/disk system. Until recently, the observed spectral energy distributions of these sources have been unresolved, i.e., the spectral energy is integrated spatially over the object. However, with the advent of new telescopes and new technology, we now have the capability to spatially resolve protostellar envelopes, especially at submillimeter wavelengths. Preliminary observations of this type have already been carried out (see, e.g., Butner et al. 1991; Yamashita et al. 1990; Walker, Adams, & Lada 1990), and much more work of this type will be done in the near future (see, e.g., the companion paper by Ladd et al. 1991b).

The principal goal of this study is to facilitate the interpretation of infrared and submillimeter observations by developing an analytic theory of emission from protostellar objects. Previous theoretical studies have solved the self-consistent radiative transfer problem for protostellar envelopes (e.g., Larson 1969; Yorke & Shutov 1981; Wolfire & Cassinelli 1986, 1987; Adams & Shu 1985, 1986). For a given protostellar configuration, these calculations numerically determine the temperature distribution and then calculate the resulting emergent spectral energy distribution. However, for spatially resolved sources (which are of interest here), the relevant physical quantity is not the integrated flux density, but rather the specific intensity I_ν convolved with the actual response function of the telescope. This convolution has been done numerically for a few protostellar sources (see Butner et al. 1991 and Walker et al. 1990 for studies of the source L1551 IRS 5 in Taurus; see Yamashita et al. 1990 for a discussion of the source GGD 27 IRS; see also Keto 1989), but a general treatment of the problem has not been done. This present study provides a general treatment of the problem by analytically determining both the specific intensity and its convolution with the response function of the telescope. In this paper, we focus on the calculation of the radiation field for a given protostellar configuration (i.e., given density and temperature distributions); notice that the previous numerical studies can be used as a starting point to determine the underlying density and temperature distributions. By providing an analytic treatment of the problem, we can isolate the functional dependence of the observed quantities on the actual physical properties of the protostellar envelope.

In order to obtain analytic results, we employ standard asymptotic methods (see, e.g., Bleistein & Handelsman 1986; de Bruijn 1981; Erdelyi 1956). By deriving analytic expressions we show the explicit dependence of the radiation field on the underlying physical parameters of the emission source. On the other hand, an analytic theory is necessarily approximate in nature. Indeed, as we discuss in some detail, the errors in our asymptotic expansions cannot be made arbitrarily small (this property is, of course, common to all asymptotic expansion analysis). Thus, care must be taken to employ our approximations only in their regime of validity.

This paper is organized as follows. We first present a formulation of the problem and review the expected protostellar configurations based on the current theory of star formation (§ 2). In § 3, we obtain an asymptotic expansion for the specific intensity I_ν; in § 4, we obtain an asymptotic expansion for the observed monochromatic luminosity (i.e., the specific intensity convolved with the response function of the telescope). The asymptotic expansions derived in §§ 3 and 4 are independent of each other and can be used for different applications. These sections are rather mathematical in nature; the observationally oriented reader may wish to skip directly to the results which

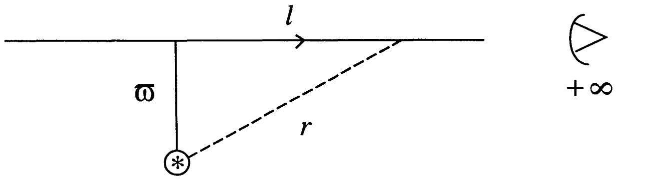

FIG. 1.—Schematic diagram showing integration path for the specific intensity integral for a given impact parameter ϖ. The observer is at spatial infinity at the far right-hand side of the diagram. The integrand is sharply peaked about the point of closest approach to the star.

are presented in equations (3.16) and (4.14). In § 5, we use these results to derive analytic expressions for the observed monochromatic luminosity ratio [the ratio $L_\nu(R)/L_\nu(0)$ of the monochromatic luminosity a distance R from the center to that in the central beam]; a more general treatment of the problem is given in Appendix B. We conclude (in § 6) with a discussion of our results and possible future applications.

2. FORMULATION OF THE PROBLEM

The specific intensity I_ν is the fundamental quantity that describes a radiation field and our first objective is to calculate I_ν for a given protostellar configuration. Theoretical considerations suggest that protostellar envelopes should be nearly spherical on the size scales probed by current observations (see, e.g., Terebey, Shu, & Cassen 1984); in our companion paper (Ladd et al. 1991b) we find that the observed aspect ratios of protostellar emission maps lie in the range 1.0–1.8 with a mean value of ~ 1.3. We therefore limit our present discussion to the case of spherical symmetry. For an observer at spatial infinity, the integral form of the specific intensity of the protostellar envelope can be written

$$I_\nu(\infty; \varpi) = \int B_\nu[T(r)] \exp(-\tau_\nu)\rho(r)\kappa_\nu \, dl , \tag{2.1}$$

where dl is the increment of path length along the ray, ρ is the density, T is the dust temperature, and κ_ν is the dust opacity (see Fig. 1). In equation (2.1) we have explicitly denoted the position of the observer as "∞"; since we are always interested in I_ν at spatial infinity, we suppress this dependence for the remainder of this paper. We have specified the direction variable by the impact parameter ϖ, which corresponds to the point of closest approach of the ray path to the center of the envelope. In the spherically symmmetric case, the impact parameter ϖ uniquely determines the ray path. Notice that we have assumed local thermodynamic equilibrium $-B_\nu[T]$ is the Planck function at dust temperature T—and that we are considering only continuum radiation. The quantity τ_ν is the optical depth between the position l along the path and the observer at infinity, i.e.,

$$\tau_\nu = \kappa_\nu \int_l^\infty \rho(r) dl' , \tag{2.2}$$

where the integral is carried out along the line of sight. Notice that the specific intensity is completely determined once the density distribution $\rho(r)$ and the temperature distribution $T(r)$ are specified. For a given specific intensity profile $I_\nu[\varpi(\boldsymbol{r}_b)]$ and a telescope with a response function $w(\boldsymbol{r}_b)$, the observed monochromatic luminosity $L_\nu(R)$ is given by the integral

$$L_\nu(R) = 4\pi \int dA \, w(\boldsymbol{r}_b) I_\nu[\varpi(\boldsymbol{r}_b)] , \tag{2.3}$$

where $\boldsymbol{R}$ is the position of the beam center (in coordinates with origin at the center of the protostellar envelope), $\boldsymbol{r}_b$ is the position vector in the plane of the sky (with origin at the beam center), $\varpi(\boldsymbol{r}_b) = |\boldsymbol{R} + \boldsymbol{r}_b|$ is the distance from the point $\boldsymbol{r}_b$ to the center of the protostellar envelope, and dA is the area element (see Fig. 2).

One basic goal of this paper is to analytically evaluate the integrals appearing in equations (2.1)–(2.3). We calculate the specific intensity I_ν analytically for a given protostellar configuration, i.e., for given density and temperature distributions. We then analytically perform the convolution of the specific intensity with the response function of a telescope. We focus our discussion on submillimeter wavelengths where emission maps of protostellar envelopes can be spatially resolved and where the emission is mostly optically thin. In the following analysis we treat the submillimeter optical depth τ_ν as a small parameter (we do not take $\tau_\nu = 0$). This assumption remains valid for the visual extinctions A_V expected for most of protostellar evolution (Adams 1990) and implies that $\exp[-\tau_\nu]$ is a slowly varying function along a ray.

The fundamental physical structure of a protostellar envelope is given by the density and temperature distributions, $\rho(r)$ and $T(r)$, respectively. The ultimate goal of this current work is twofold: We want to provide a general basis for interpreting the observed spatial distribution of protostellar emission in order to ascertain the actual structure in an unbiased manner. In addition, we want to compare observational results with the current protostellar theory. In order to achieve both of these goals, we introduce purely *parametric* power-law forms for the density and the temperature distributions, i.e.,

$$\rho(r) = \rho_0 \left(\frac{r_0}{r}\right)^p \quad \text{and} \quad T(r) = T_0 \left(\frac{r_0}{r}\right)^q , \tag{2.4}$$

where r_0 is some fiducial radius and ρ_0 and T_0 are the values of the density and temperature, respectively, at r_0. By using the forms given in equation (2.4), we can calculate observable quantities in terms of the basic physical parameters (p, q, T_0, ρ_0) of the protostellar envelope. In a fully self-consistent theory, the density and temperature distributions are determined by the initial conditions (and by the time t since the onset of protostellar collapse). As we discuss in the following sections, however, the current theory suggests that the density and temperature distributions are nearly power laws (especially on the size scales probed by the observations). As a result, one can think of the self-consistent theory as providing definite values for the parameters appearing in equation (2.4).

2.1. *Observational Considerations*

For this paper, the wavelength range of interest is approximately 100 μm $\leq \lambda \leq$ 1100 μm. At shorter wavelengths, pro-

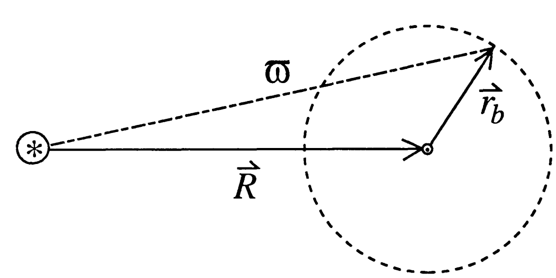

FIG. 2.—Schematic diagram showing integration variables for the monochromatic luminosity integral for a given distance R of the beam center. The plane of the figure corresponds to the plane of the sky.

tostellar sources are generally not well resolved by present-day telescopes; at longer wavelengths, the emitted flux density becomes very small and measurements with high signal-to-noise ratios become difficult to make. In this given wavelength range, telescopes generally have response functions (beam profiles) which can be modeled with simple Gaussian profiles. In this paper, we thus consider the response function $w(r_b)$ of the telescope to have a simple Gaussian form

$$w(r_b) = \mathcal{N} \exp\left[-r_b^2 4 \ln(2)/B^2\right] , \quad (2.5)$$

where B is the physical distance corresponding to the full width at half-maximum (FWHM) of the beam pattern and where $\mathcal{N}$ is the normalization constant. Present-day telescopes can achieve an angular resolution in the range 10″–60″ (these values correspond to the FWHM of the telescope beam). At the distance of nearby molecular clouds (~ 150 pc), this range of angular scales corresponds to physical size scales B in the range

$$B = (2.25 \rightarrow 13.5) \times 10^{16} \text{ cm} . \quad (2.6)$$

It is obvious that observations cannot probe structure on size scales much smaller than B—one result of our analysis is a quantification of this statement. We are thus interested in the predictions of the protostellar theory on size scales $\mathcal{O}(10^{16}$ cm) and larger; in the following subsections we review these predictions.

2.2. *The Density Distribution*

In the current theory of star formation, the density distribution is calculated from the equations of motion for a collapsing gaseous cloud. For protostars with relatively low mass ($M < 2\ M_\odot$), radiation pressure produces a negligible effect on the collapse flow and the dynamics are decoupled from the radiation field; the physical structure of the protostellar envelope—and especially the relevant size scales in the problem—can thus be determined directly from an a priori dynamical calculation.

For the simplest case of a spherical (nonrotating) and isothermal cloud core, the initial (unstable) equilibrium density distribution of the core has the form

$$\rho(r) = \frac{a^2}{2\pi G} \frac{1}{r^2} , \quad (2.7)$$

where a is the isothermal sound speed. The collapse of a core with the initial configuration (2.7) proceeds in a self-similar manner; this self-similar collapse proceeds from inside-out, with the central portions falling first and subsequent outer layers following as an expansion wave propagates outward at the sound speed (see Shu 1977). The region outside of the collapse boundary $r_H = at$ is unaffected by the collapse and retains the initial density distribution (2.7). Notice that this solution is valid if and only if the head of the expansion wave r_H lies within the effective boundary of the core $r_{\rm core}$; the boundary $r_{\rm core}$ can be simply defined as the (outer) radius at which the initial density distribution of equation (2.7) no longer applies.

In the inner part of the collapse, the gravitational force dominates over the thermal pressure and the material is essentially in free-fall; in this region, the density distribution approaches the form

$$\rho = C r^{-3/2} , \quad \text{where} \quad C \equiv \frac{m_0 a^3}{4\pi(2G^3 M)^{1/2}} , \quad (2.8)$$

and the dimensionless constant $m_0 = 0.975$ (Shu 1977). The form of equation (2.8) for the density distribution is valid in the regime $R_C \ll r \ll r_H$, where R_C is the centrifugal radius (Terebey et al. 1984) defined by

$$R_C \equiv \frac{\Omega^2 G^3 M^3}{16 a^8} . \quad (2.9)$$

For typical protostellar sources the radius R_C is generally of order 10^{14}–10^{15} cm (~ 10–100 AU; see Adams et al. 1987), which is much smaller than the size scale B probed by present observations. The outer radius R_D of the circumstellar disk is expected to be approximately given by R_C so that the entire star/disk system has a size scale much smaller than B. The spherical free-fall form of equation (2.8) thus describes the density distribution for most radii of observational interest (i.e., $p \approx 3/2$); however, for the large end of the size range, the density distribution approaches the equilibrium form of equation (2.7). Thus, for the size scales of interest in this paper, we expect that

$$\frac{3}{2} \le p \le 2 \quad (2.10)$$

will be the appropriate range for the power-law index p of the density distribution.

For radii much less than the centrifugal radius (2.9) the collapse flow is highly nonspherical and nearly ballistic (pressure-free) in nature. The temperature of the envelope increases inward until the temperature is too hot for dust grains to remain in their solid phase; the dust grains then sublimate at a well-defined dust destruction radius r_d (Stahler, Shu, & Taam 1980), which is of $\mathcal{O}(10^{12}$ cm) for protostars of solar-type masses (Adams & Shu 1986). The inner boundary of the collapse flow is given by the stellar surface, which has a radius $R_* \sim 10^{11}$ cm for protostars of solar-type masses (e.g., Stahler et al. 1980). Putting all of the size scales in the problem together, we thus obtain the ordering

$$R_* \ll r_d \ll R_C \ll B \ll r_H \ll r_{\rm core} . \quad (2.11)$$

Notice that most of the size scales appearing in the above ordering depend on the mass M that has fallen to the central star/disk system; however, this mass is within a factor of a few of the final mass for most of the time spent in the embedded phase. Thus, this ordering is expected to be valid for a substantial portion of the protostellar (embedded) phase of evolution. However, for the youngest objects and the largest beam sizes, we can have $B \sim r_H$.

2.3. *The Temperature Distribution*

In the outer portion of the protostellar envelope, we can analytically estimate the temperature distribution. This derivation, which is given in Appendix A, shows that the temperature distribution in the outer envelope is nearly a power-law (in the radial coordinate) if the dust opacity also has a power-law form at low frequencies,

$$\kappa_\nu = A \nu^\beta . \quad (2.12)$$

Most estimates of interstellar dust opacities (see, e.g., Draine & Lee 1984; Hildebrand 1983) suggest that the power-law form of equation (2.12) is valid at submillimeter wavelengths (low frequencies) and that the index β lies in the range $1 \le \beta \le 2$. Using the expected form of the temperature distribution (see eq. [A5]), we obtain an estimate for the power-law index q:

$$q = \frac{2}{4+\beta} \Rightarrow \frac{1}{3} \le q \le \frac{2}{5}, \quad (2.13)$$

where we have used the expected range $1 \le \beta \le 2$ in obtaining the second relation.

3. ASYMPTOTIC EXPANSION FOR THE SPECIFIC INTENSITY INTEGRAL

In this section, we derive an analytic form for the specific intensity of a protostellar envelope. Once the temperature and density distributions have been specified, we can write the specific intensity in the form

$$I_\nu = \frac{2h\nu^3}{c^2} \kappa_\nu \varpi \rho(\varpi) \mathscr{I}(\varpi), \quad (3.1)$$

where we have written the integral in dimensionless form through

$$\mathscr{I}(\varpi) = \int_{-\infty}^{\infty} ds \left(\frac{\varpi}{r}\right)^p \frac{1}{e^x - 1} \exp(-\tau_\nu), \quad (3.2)$$

where we have defined a dimensionless variable of integration $s \equiv l/\varpi$, and where x is defined by

$$x \equiv \frac{h\nu}{kT(r)} = \frac{h\nu}{kT_0}\left(\frac{r}{r_0}\right)^q. \quad (3.3)$$

We want to approximate the integral $\mathscr{I}$ using standard asymptotic methods (see, e.g., Bleistein & Handelsman 1986; de Bruijn 1981). Since we are interested in emission in the optically thin regime, we consider the factor $f(s) \equiv \exp(-\tau_\nu)$ to be a slowly varying function of the variable s. Notice that in the extreme optically thin limit $f(s)$ becomes unity; here, however, we obtain a slightly better approximation by retaining the optical depth factor and considering it as slowly varying. We then define a new function Φ through the *Ansatz*

$$e^{-\Phi} \equiv \left(\frac{\varpi}{r}\right)^p \frac{1}{e^x - 1}, \quad \text{or} \quad \Phi = p \ln(r/\varpi) + \ln(e^x - 1), \quad (3.4)$$

which is to be considered as a function of the variable of integration s. Using both formal and intuitive arguments, it is straightforward to show that the maximum of the integrand [the minimum of $\Phi(s)$] occurs at $s = 0$, i.e., the point of closest approach of the ray to the origin. In obtaining an asymptotic approximation for the integral $\mathscr{I}$, we are assuming that most of the contribution of the integral occurs near the maximum at $s = 0$, i.e., we assume that the function $e^{-\Phi}$ is sharply peaked about $s = 0$. This assumption is the weakest in the low-frequency limit where $\Phi = (p + q)\ln(r/\varpi) + constant$. As we show below, in this limiting case we obtain an asymptotic series in the parameter $\lambda = (p + q)$; this expansion is valid in the limit $\lambda \to \infty$.

Notice that the function Φ is an *even* function of s, i.e., it is symmetric about the point $s = 0$. If we then expand the function Φ about the point $s = 0$, we obtain only the even terms:

$$\begin{aligned}\Phi(s) &= \Phi_0 + \frac{1}{2}\Phi_0'' s^2 + \frac{1}{24}\Phi_0^{iv} s^4 + \dots \\ &= \ln(e^{x_0} - 1) + \frac{1}{2}(p + qQ)s^2 \\ &\quad - \frac{1}{8}[2(p + qQ) + q^2 Q(Q - 1 - x_0]s^4 + \dots, \quad (3.5)\end{aligned}$$

where the subscript 0 means that the function is to be evaluated at $s = 0$ ($r = \varpi$), e.g., $x_0 \equiv h\nu/kT(\varpi)$. The superscripts denote derivatives of Φ with respect to s in obvious notation. We have also defined a new function $Q(x)$ through

$$Q(x) \equiv \frac{xe^x}{e^x - 1}, \quad (3.6)$$

where Q is to be evaluated at $x = x_0$ in equation (3.5). Notice that $Q \to 1$ in the limit of small $x \ll 1$ and that $Q \to x$ in the opposite limit $x \gg 1$. Similarly, we can expand the function $f(s)$ about the point $s = 0$:

$$f(s) = f_0 + f_0' s + \frac{1}{2} f_0'' s^2 + \dots. \quad (3.7)$$

Since we need to treat the region $s < 0$ slightly differently than the region of $s > 0$, it is useful to separate the integral $\mathscr{I}$ into two separate parts, i.e., let

$$\mathscr{I} = \mathscr{I}_A + \mathscr{I}_B, \quad (3.8a)$$

where

$$\mathscr{I}_A = \int_{-\infty}^{0} ds\, e^{-\Phi} f(s) \quad \text{and} \quad \mathscr{I}_B = \int_0^{\infty} ds\, e^{-\Phi} f(s). \quad (3.8b)$$

We now change variables of integration from s to τ, where τ is the defined through

$$\tau \equiv \Phi(s) - \Phi_0. \quad (3.9)$$

In order to evaluate the integrals $\mathscr{I}_A$ and $\mathscr{I}_B$, we need to evaluate the quantity $G(\tau)$ which is defined by

$$G(\tau) \equiv \frac{ds}{d\tau} = \left(\frac{d\Phi}{ds}\right)^{-1}. \quad (3.10)$$

We thus obtain

$$\mathscr{I}_A = -e^{-\Phi_0} \int_0^{\infty} d\tau\, e^{-\tau} f[s(\tau)] G(\tau), \quad (3.11a)$$

$$\mathscr{I}_B = e^{-\Phi_0} \int_0^{\infty} d\tau\, e^{-\tau} f[s(\tau)] G(\tau). \quad (3.11b)$$

In order to evaluate the integrals in equations (3.11), we must write s in terms of τ by using equation (3.5):

$$\Phi_0^{iv} s^4 + 12\Phi_0'' s^2 - 24\tau = 0, \quad (3.12)$$

which is correct up to $\mathcal{O}(s^6)$. Notice that equation (3.12) is a quadratic in s^2, so that two roots exist for s^2; we can distinguish the physical root by requiring that $s \to 0$ as $\tau \to 0$. Notice that we are still left with a sign ambiguity for s itself; for $s < 0$ (as in $\mathscr{I}_A$) we take the negative root, whereas for $s > 0$ (as in $\mathscr{I}_B$) we take the positive root. We can thus write expansions for the integrand $f(s[\tau])G(\tau)$ for the region $s > 0$

$$f(s[\tau])G(\tau) = (2\Phi_0''\tau)^{-1/2} \times \left\{f_0 + f_0'\left(\frac{2\tau}{\Phi_0''}\right)^{1/2} + \tau\left[\frac{f_0''}{\Phi_0''} - \frac{f_0 \Phi_0^{iv}}{4(\Phi_0'')^2}\right] + \dots\right\}, \quad (3.13a)$$

and for the region $s < 0$

$$-f(s[\tau])G(\tau) = (2\Phi_0''\tau)^{-1/2} \times \left\{f_0 - f_0'\left(\frac{2\tau}{\Phi_0''}\right)^{1/2} + \tau\left[\frac{f_0''}{\Phi_0''} - \frac{f_0 \Phi_0^{iv}}{4(\Phi_0'')^2}\right] + \cdots\right\}. \quad (3.13b)$$

Collecting all of the above results and evaluating the integrals over τ (which are now simply gamma functions; see e.g., Abramowitz & Stegun 1965), the asymptotic expansion for the integral $\mathscr{I}$ takes the form

$$\mathscr{I}(\varpi) = f_0 e^{-\Phi_0}\left(\frac{2\pi}{\Phi_0''}\right)^{1/2}\left[1 + \frac{1}{2\Phi_0''}\left(\frac{f_0''}{f_0} - \frac{\Phi_0^{iv}}{4\Phi_0''}\right) + \cdots\right]. \quad (3.14)$$

In terms of the original parameters of the problem we can write

$$\mathscr{I}(\varpi) = (2\pi)^{1/2}(e^{x_0} - 1)^{-1}(p + qQ)^{-1/2} \exp\left[-\tau_\nu(\varpi)\right] \times \left[1 + \frac{6 - 3qP + 4(\rho\kappa_\nu\varpi)^2}{8(p + qQ)} + \cdots\right], \quad (3.15a)$$

where we have defined a new function through

$$P \equiv \frac{qQ}{p + qQ}(1 + x - Q). \quad (3.15b)$$

Notice that P is slowly varying and is confined to the range $0 \le P \le 1$. We thus obtain the analytic estimate for the specific intensity, which takes the form

$$I_\nu(\varpi) = (2\pi)^{1/2}\kappa_\nu \varpi\rho(\varpi)B_\nu[T(\varpi)](p + qQ)^{-1/2} \exp\left[-\tau_\nu(\varpi)\right] \times \left[1 + \frac{6 - 3qP + 4(\rho\kappa_\nu\varpi)^2}{8(p + qQ)} + \cdots\right], \quad (3.16)$$

where all the functions are to be evaluated at $r = \varpi$. Equation (3.16) represents the first two terms of an asymptotic series, which is essentially an expansion in the parameter $\lambda_I \equiv (p + qQ)$ and becomes exact in the limit $\lambda_I \to \infty$. This asymptotic expansion has the form expected from application of *Laplace's method* with λ_I considered as a large parameter (Bleistein & Handelsman 1986). In order to complete the specification of $I_\nu(\varpi)$, we must evaluate the integral for the optical depth $\tau_\nu(\varpi)$, which can be written as

$$\tau_\nu(\varpi) = \kappa_\nu \rho(\varpi)\varpi \int_0^\infty (1 + s^2)^{-p/2} ds = \kappa_\nu \rho(\varpi)\varpi \frac{\sqrt{\pi}}{2}\frac{\Gamma[(p - 1)/2]}{\Gamma(p/2)}, \quad (3.17)$$

where we have written the integral in terms of gamma functions (see, e.g., Abramowitz & Stegun 1965). For our expected value of $p = 3/2$, the numerical coefficient in equation (3.17) is 2.622.

One way to characterize the specific intensity profile is by defining an equivalent power-law index μ through

$$\mu \equiv -\frac{\varpi}{I_\nu(\varpi)}\frac{dI_\nu}{d\varpi}, \quad (3.18)$$

which is generally a function of both the impact parameter ϖ and the frequency ν. Using equation (3.16) we find that μ is given by

$$\mu = -1 + (p + qQ) + \frac{q}{2}P - (p - 1)\tau_\nu + \mathscr{O}\left(\frac{\tau_\nu^2}{\lambda_I}\right) + \mathscr{O}\left(\frac{1}{\lambda_I^2}\right), \quad (3.19)$$

where we have neglected higher order terms. Notice that for most cases of interest the first two terms dominate, i.e., $\mu \approx (p + qQ) - 1 = \lambda_I - 1$. As $x = h\nu/kT$ becomes larger than unity, μ becomes large, i.e., the specific intensity falls off steeply with increasing impact parameter.

3.1. *Low-Frequency Limit*

At this point, it is useful to consider the integral $\mathscr{I}$ in the limits of low-frequency ($x \to 0$) *and* low optical depth ($\tau_\nu \to 0$). In this limit, $\lambda_I = (p + q)$, and our asymptotic expansion (eq. [3.15]) can be written in the form

$$\mathscr{I}(\lambda_I) = \frac{kT_0}{h\nu}\left(\frac{r_0}{\varpi}\right)^q\left(\frac{2\pi}{\lambda_I}\right)^{1/2}\left(1 + \frac{3}{4\lambda_I} + \cdots\right). \quad (3.20)$$

Since $p + q$ is generally ~ 2 or so, we expect that this expansion is fairly approximate in the low-frequency limit. However, in this limit we can rewrite the integral $\mathscr{I}$ as

$$\mathscr{I}(\lambda_I) = \frac{1}{x_0}\int_{-\infty}^{\infty} ds(1 + s^2)^{-\lambda_I/2} = \frac{\sqrt{\pi}}{x_0}\frac{\Gamma[(\lambda_I - 1)/2]}{\Gamma(\lambda_I/2)}, \quad (3.21)$$

where we have evaluated the integral in terms of gamma functions. Notice that the validity of this expression is restricted to the region of parameter space where $\lambda_I > 1$ (the integral $\mathscr{I}$ diverges for $\lambda_I \le 1$). For the representative case $\lambda_I = p + q = 2$, the numerical coefficient for the exact integral is π (from eq. [3.21]) and the coefficient for our expansion is $11(\pi^{1/2})/8$ (where we have used the first two terms in eq. [3.20]). The relative error for this particular case is thus 22%. When the low-frequency limit does not apply, the integrand of $\mathscr{I}$ is more sharply peaked about $s = 0$ and our asymptotic expansion (eq. [3.16]) produces a better approximation. Notice also that in the low-frequency limit, all of the error is in the coefficient and not in the functional dependence of I_ν (i.e., we get $I_\nu \propto \varpi^{1-p-q}$ in both cases).

4. CONVOLUTION OF THE SPECIFIC INTENSITY WITH A GAUSSIAN BEAM

In this section, we derive an asymptotic expansion which convolves a given specific intensity profile $I_\nu(\varpi)$ with a (Gaussian) telescope response function. If we use the results of § 3 to specify $I_\nu(\varpi)$, we can estimate the expected monochromatic luminosity as a function of protostellar parameters. Although the results of this section are derived in the context of protostellar emission, the resulting asymptotic expansion can be used in other astrophysical applications.

For a telescope with a normalized response function $w(\boldsymbol{r}_b)$, the observed monochromatic luminosity $\mathscr{L}_\nu(R)$ from the protostellar envelope is given by the integral

$$\mathscr{L}_\nu(R) = 4\pi \int dA\, w(\boldsymbol{r}_b)I_\nu[\varpi(\boldsymbol{r}_b)], \quad (4.1)$$

where the symbols are defined as in equation (2.3). For the size scales B corresponding to most observing beams of interest, the central star/disk system is pointlike, i.e., $B \gg R_D$. To obtain the total observed monochromatic luminosity, we must also include the contribution from the source

$$L_\nu^C(R) = \int dA\, w(\boldsymbol{r}_b)L_{\nu c}\, e^{-\tau_{\nu c}}\delta^2(\boldsymbol{r}_b + \boldsymbol{R}) = L_{\nu c}\, e^{-\tau_{\nu c}}w(R), \quad (4.2)$$

where $L_{\nu c}$ is the intrinsic monochromatic luminosity from the central star/disk system, $\tau_{\nu c}$ is the total optical depth through the protostellar envelope, and $\delta^2(x)$ is the Dirac δ-function in two dimensions. Since the central source contribution is completely specified by equation (4.2) for a given central source, the remainder of this section focuses on the calculation of an asymptotic approximation to the contribution of the protostellar envelope (eq. [4.1]).

We begin by defining a dimensionless parameter λ_B through

$$\lambda_B \equiv 8\ln(2)R^2/B^2 , \quad (4.3)$$

where B is the length corresponding to the FWHM of the beam pattern (see § 2). Let (x, y) be the coordinates in the plane of the sky centered on the protostellar envelope. Since the envelope is assumed to be spherical, without loss of generality we can take the center of the observing beam to lie along the x-axis and have the position $(R, 0)$. We then define dimensionless coordinates (ξ, η) which are centered on the beam position:

$$\xi = (x - R)/R \quad \text{and} \quad \eta = y/R . \quad (4.4)$$

The integral for $\mathscr{L}_\nu$ can then be written

$$\mathscr{L}_\nu = \mathscr{N} 4\pi R^2 \int_{-\infty}^{\infty} d\xi \int_{-\infty}^{\infty} d\eta \exp\left[-\frac{\lambda_B}{2}(\xi^2+\eta^2)\right] I_\nu(\xi, \eta) . \quad (4.5)$$

We now have the integral in proper form to perform an asymptotic expansion. Following Bleistein & Handelsman (1986), we write our first approximation of I_ν in the form

$$I_\nu(\xi, \eta) = I_\nu(0, 0) + \boldsymbol{\xi} \cdot \boldsymbol{H}_0 , \quad (4.6)$$

where $\boldsymbol{\xi}$ is the two-dimensional vector (ξ, η), and $\boldsymbol{H}_0$ is a two-dimensional vector which can be chosen in a variety of ways. However, we will see later that certain advantages arise if we adopt the judicious choice

$$H_{0\xi} = \frac{1}{\xi}\left[I_\nu(\xi, \eta) - I_\nu(0, \eta)\right] , \quad (4.7a)$$

$$H_{0\eta} = \frac{1}{\eta}\left[I_\nu(0, \eta) - I_\nu(0, 0\right] . \quad (4.7b)$$

Notice that the form (4.7) is slightly different than the naive choice $H_{0\xi} = (dI_\nu/d\xi)_0$ and $H_{0\eta} = (dI_\nu/d\eta)_0$. In particular, substitution of equations (4.7) into equation (4.6) shows that the equality is *exact* (rather than an approximation correct to first order in ξ and η). If we insert the forms from equations (4.6)–(4.7) for I_ν and $\boldsymbol{H}_0$ in equation (4.5), we obtain

$$\mathscr{L}_\nu/\mathscr{N} 4\pi R^2 = I_0(0, 0) \int_{-\infty}^{\infty} d\xi \int_{-\infty}^{\infty} d\eta \exp\left[-\frac{\lambda_B}{2}(\xi^2+\eta^2)\right] + \frac{1}{\lambda_B} \int_{-\infty}^{\infty} d\xi \int_{-\infty}^{\infty} d\eta \exp\left[-\frac{\lambda_B}{2}(\xi^2+\eta^2)\right] I_1(\xi, \eta) , \quad (4.8)$$

where we have used the divergence theorem (the resulting surface term vanishes) and we have defined

$$I_1 \equiv \nabla \cdot \boldsymbol{H}_0 . \quad (4.9)$$

If we repeat this process N times, we obtain an asymptotic expansion of the form

$$\mathscr{L}_\nu = \mathscr{N} 4\pi R^2 \sum_{j=0}^{N-1} \lambda_B^{-j} I_j(0, 0) \int_{-\infty}^{\infty} d\xi \int_{-\infty}^{\infty} d\eta \times \exp\left[-\frac{\lambda_B}{2}(\xi^2+\eta^2)\right] + \mathscr{O}(\lambda_B^{-N}) , \quad (4.10)$$

where the functions I_j are defined recursively through the relations

$$I_j(\xi, \eta) = I_j(0, 0) + \boldsymbol{\xi} \cdot \boldsymbol{H}_j(\xi, \eta) , \quad (4.11a)$$

$$I_{j+1}(\xi, \eta) = \nabla \cdot \boldsymbol{H}_j(\xi, \eta) . \quad (4.11b)$$

(Notice that the notation "$\boldsymbol{H}_j$" refers to the jth vector in a series and *not* to the jth component of a vector.) Using the definitions (4.11) in conjunction with Lemma 8.3.2 of Bleistein & Handelsman (1986), we can evaluate the functions $I_j(0, 0)$ in terms of the original function $I_\nu(\varpi)$. This lemma implies that

$$I_j(0, 0) = \frac{1}{2^j j!} \Delta_2^j I_\nu \Big|_{(0,0)} , \quad (4.12)$$

where Δ_2 is the two-dimensional Laplacian operator, i.e.,

$$\Delta_2 \equiv \frac{\partial^2}{\partial\xi^2} + \frac{\partial^2}{\partial\eta^2} . \quad (4.13)$$

We thus obtain the expansion

$$\mathscr{L}_\nu(R) = \mathscr{N} \frac{8\pi^2 R^2}{\lambda_B} \sum_{j=0}^{N-1} \frac{1}{(2\lambda_B)^j j!} \Delta_2^j I_\nu \Big|_{(0,0)} + \mathscr{O}(\lambda_B^{-N}) . \quad (4.14)$$

Notice that we have not written the expansion in equation (4.14) as an infinite series, but rather as the $N - 1$th partial sum with an error term $\mathscr{O}(\lambda_B^{-N})$. An infinite series would be meaningless in this context because the series need not converge (this property is a well-known aspect of asymptotic analysis; see, e.g., Bleistein & Handelsman 1986). This expansion approaches the exact integral (eq. [4.1]) only in the limit $\lambda_B \to \infty$. For any finite λ_B, the approximation of equation (4.14) becomes better (closer to the exact result) for the first N_C terms and diverges with the addition of higher order terms; here, the integer N_C is the largest integer for which the ratio of successive terms is less than or equal to 1.

For any given specific intensity profile I_ν, equation (4.14) provides the desired asymptotic expansion for the observed emission $\mathscr{L}_\nu(R)$. The derivation leading to equation (4.14) does not depend on the assumption of spherical symmetry and hence the expansion is valid for any function $I_\nu(\xi, \eta)$. We can, however, use the (spherical) profile $I_\nu(\varpi)$ derived in the previous section to specify I_ν in terms of the temperature and density distributions. Finally, we should remark that the expansion of equation (4.14) is not applicable for the central beam (where $R = 0 = \lambda_B$); for this case, the integral of equation (4.1) must be solved by different methods, as we discuss below (see also Appendix B).

5. MONOCHROMATIC LUMINOSITY PROFILES

For observed maps of protostellar emission, one of the most well defined physically measurable quantities is the monochromatic luminosity profile $L_\nu(R)/L_\nu(0)$. Since we are considering the ratio $L_\nu(R)/L_\nu(0)$, any errors associated with the absolute calibrations are eliminated. In this section, we combine the results of §§ 3 and 4 to derive an analytic expression for the monochromatic luminosity profile as a function of protostellar parameters.

To begin, we must evaluate the expansion for $\mathscr{L}_\nu(R)$ given by equation (4.14) above (here we consider only the first three terms). Since the specific intensity I_ν is a function of ϖ only, we can write the Laplacian operator (see eq. [4.13]) as

$$\Delta_2 = R^2\left\{\frac{d^2}{d\varpi^2} + \frac{1}{\varpi}\frac{d}{d\varpi}\right\} . \quad (5.1)$$

The action of the Laplacian operator on the specific intensity then becomes

$$\Delta_2 I_\nu \Big|_{(0,0)} = \left\{\mu^2 - R \frac{d\mu}{d\varpi}\Big|_R\right\} I_\nu(R) , \qquad (5.2a)$$

$$\Delta_2^2 I_\nu \Big|_{(0,0)} = \left[\mu^2(\mu+2)^2 - R \frac{d\mu}{d\varpi}\Big|_R \times (6\mu^2 + 8\mu + 1) + 3\left(R \frac{d\mu}{d\varpi}\Big|_R\right)^2 + R^2 \frac{d^2\mu}{d\varpi^2}\Big|_R (1 + 4\mu) - R^3 \frac{d^3\mu}{d\varpi^3}\Big|_R\right] I_\nu(R) , \qquad (5.2b)$$

where we have written the above expressions in terms of the index μ defined by equation (3.19). The above forms are somewhat complicated. Fortunately, however, the index μ is a slowly varying function; for example, if we take the representative values $p = 3/2$ and $q = 2/5$, then the quantity $(R d\mu/d\varpi)_R/\mu^2$ obtains a maximum value (over all x) of ~ 0.13. The variation of μ thus represents (at most) a 13% correction to the $\mathcal{O}(\lambda_B^{-1})$ term in the expansion and can be ignored to a reasonable degree of accuracy. Using these results in the equation (4.14), we obtain the expansion for the protostellar envelope contribution:

$$\mathscr{L}_\nu(R) = \mathscr{N} \frac{\pi^2 B^2}{\ln(2)} I_\nu(R) \left[1 + \frac{\mu^2}{2\lambda_B} + \frac{\mu^2(\mu+2)^2}{8\lambda_B^2} + \mathcal{O}\left(\frac{1}{\lambda_B^3}\right)\right] , \qquad (5.3)$$

which is valid in the regime $\lambda_B \gg 1$, i.e., $R \gg B/(8 \ln 2)^{1/2}$. Notice that the expansion in equation (5.3) contains two separate sources of error. The first source of error is that due to the asymptotic expansion itself, which has three terms in the present form. For a "typical" case with $\mu = 1$ and $R = B$, this error is $\sim 4\%$. The second source of error is associated with the approximation of ignoring the derivatives of μ (notice that we are effectively assuming that I_ν is a power law in ϖ). As discussed above, if we included the full radial dependence of μ, we would obtain a correction of order $10\lambda_B^{-1}\%$.

We must now calculate the monochromatic luminosity $\mathscr{L}_\nu(R = 0)$ of the central beam (for the protostellar envelope). Since, to leading order, we can ignore the derivatives of μ in the expansion for $\mathscr{L}_\nu(R)$, we determine the expected monochromatic luminosity profiles for a specific intensity I_ν with a power-law form, i.e., we take I_ν to be given by

$$I_\nu(\varpi) = I_{\nu 0}\left(\frac{r_d}{\varpi}\right)^m \quad \text{for} \quad \varpi > r_d , \qquad (5.4a)$$

$$I_\nu(\varpi) = I_{\nu 0} \quad \text{for} \quad \varpi \le r_d , \qquad (5.4b)$$

where r_d is the dust destruction radius. The end result of this analysis is a determination of the power-law index m, which can be identified with the equivalent power-law index μ of the specific intensity (see eq. [3.19]). Notice, however, that taking I_ν to be purely a power law (as in eq. [5.4]) provides a reasonable approximation for "long" wavelengths (typically in the range $\lambda \geq 350$ μm); for shorter wavelengths, the approximation of equation (5.4) begins to break down for the central beam. In Appendix B we give a more general treatment of the central beam integral.

With the form equation (5.4) for the specific intensity, we have

$$\mathscr{L}_\nu(0) = \mathscr{N} \frac{\pi^2 B^2}{\ln(2)} I_{\nu 0}\left(1 - e^{-z_d^2} + 2 z_d^m \int_{z_d}^{\infty} dz\, z^{1-m} e^{-z^2}\right) , \qquad (5.5)$$

where we have defined a new variable z through

$$z^2 \equiv 4 \ln(2) \varpi^2/B^2 . \qquad (5.6)$$

The parameter z_d is simply z evaluated at $\varpi = r_d$; notice that for typical values of B and r_d, we have $z_d = \mathcal{O}(10^{-8})$. If we evaluate the integral in the above expression by writing it as a power series in z_d, we obtain the monochromatic luminosity of the central beam

$$\mathscr{L}_\nu(0) = \mathscr{N} \frac{\pi^2 B^2}{\ln(2)} I_{\nu 0} \left[1 - e^{-z_d^2} + z_d^m \Gamma(1 - m/2) - 2 \sum_{k=0}^{\infty} \frac{(-1)^k}{k!} \frac{z_d^{2k+2}}{2k + 2 - m}\right] \qquad (5.7)$$

Notice that the power series in z_d is convergent and we can thus approximate the original integral to any desired accuracy.

We can now calculate the ratio of the monochromatic luminosity at some radius $R \geq B$ to the central value $L_\nu(0)$. This monochromatic luminosity ratio $L_\nu(R)/L_\nu(0)$ is a well-defined observational quantity. We first consider the simplest case in which the central source contribution (see eq. [4.2]) is negligible, i.e., $L_\nu = \mathscr{L}_\nu$; if we identify μ with m, we obtain

$$\frac{L_\nu(R)}{L_\nu(0)} = \left(\frac{2}{\lambda_B}\right)^{m/2} \frac{1}{\Gamma(1 - m/2)} \times \left[1 + \frac{m^2}{2\lambda_B} + \frac{m^2(m+2)^2}{8\lambda_B^2} + \mathcal{O}\left(\frac{1}{\lambda_B^3}\right) + \mathcal{O}(z_d^{2-m})\right] , \qquad (5.8)$$

where the R dependence of the above equation is contained in the parameter $\lambda_B = 8 \ln(2) R^2/B^2$. Monochromatic luminosity profiles for various power-law indices m are shown in Figure 3. The approximations leading to equation (5.8) are valid for large radii ($R \geq B$) and long wavelengths (typically $\lambda \geq 350$

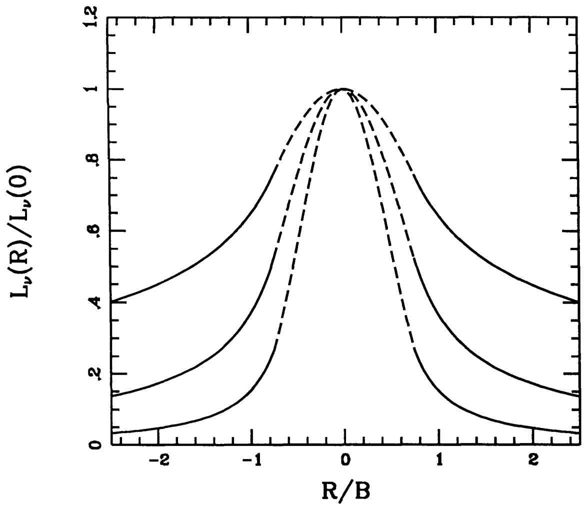

FIG. 3.—Monochromatic luminosity profiles for varying effective power-law indices m of the specific intensity profile. The solid curves show profiles for $m = 1/2$ (*top curve*), $m = 1$ (*center curve*), and $m = 3/2$ (*bottom curve*). The dotted portions of the curves are heuristic and correspond to beam offset radii R which are too small for the asymptotic theory to be valid.

μm). At short wavelengths, the approximation of equation (5.4) breaks down and the central beam integral can no longer be approximated with a single power law [when $x(R) = h\nu/kT(R) = 1$, our approximation is good to a few percent; as $x(R)$ increases to ~ 4, the value of μ increases to 2, and the central beam integral diverges]. Notice that the result of equation (5.3) for the numerator $\mathscr{L}_\nu(R)$ is more robust than equation (5.7) for the denominator $\mathscr{L}_\nu(0)$.

Since the only free parameter in the ratio is the power-law index m, equation (5.8) can be solved for m which thus defines an *equivalent power-law index* for the specific intensity. Notice that in the limit $m \to 0$ we recover the expected result that $L_\nu(R)/L_\nu(0) \to 1$; in the limit $m \to 2$, we obtain $L_\nu(R)/L_\nu(0) \to 0$. Thus, for any observed ratio $L_\nu(R)/L_\nu(0)$, equation (5.8) defines an equivalent power-law index $m \in [0, 2]$. In the regime where the approximation of equation (5.4) is valid, we can identify the index m with μ. We thus obtain a relationship between directly measurable quantities [i.e., $L_\nu(R)/L_\nu(0)$] and the basic physical parameters of the protostellar envelope (p, q, and T_0).

We now consider the case in which the central star/disk system makes a substantial contribution to the monochromatic luminosity. In this case, let us write the central source contribution in terms of the ratio γ_ν defined by

$$\gamma_\nu \equiv \frac{L_{\nu c} e^{-\tau_{\nu c}} w(0)}{\mathscr{L}_\nu(0)} , \tag{5.9}$$

which is independent of R but is a function of frequency ν. The monochromatic luminosity profile can then be written

$$\frac{L_\nu(R)}{L_\nu(0)} = \frac{1}{1+\gamma_\nu} \frac{(2/\lambda_B)^{m/2}}{\Gamma(1-m/2)} \times \left[1 + \frac{m^2}{2\lambda_B} + \frac{m^2(m+2)^2}{8\lambda_B^2}\right] + \frac{\gamma_\nu}{1+\gamma_\nu} e^{-\lambda_B/2} . \tag{5.10}$$

Notice that in this form the monochromatic luminosity profile has two unspecified parameters: m and γ_ν. Thus, measurements at two different radii $R > B$ must be performed in order to estimate the effective power-law index m and the relative contribution γ_ν of the central star/disk system.

Notice that to leading order the monochromatic luminosity profile has a power-law form $L_\nu(R)/L_\nu(0) \propto R^{-m}$; the expected distribution is thus scale-free. Keep in mind, however, that the above forms are valid only in the spatial regime defined by $B \ll R \ll r_{\rm core}$. At the inner size scale, our asymptotic expansion becomes invalid (the expansion parameter λ_B becomes small) and the ratio must approach unity. The outer size scale, which we have denoted as $r_{\rm core}$, is determined by the boundary of the molecular cloud core. This boundary is roughly defined as the radius at which the density distribution flattens out sufficiently that $\rho(r)$ can no longer be described by a power-law (and hence our approximations break down). Although this size scale is not observationally well determined, $r_{\rm core}$ is expected to be $\mathscr{O}(1\ {\rm pc})$. In practice, however, flux density measurements at distances of order $r_{\rm core}$ cannot be performed with an appreciable signal-to-noise ratio; the effective outer radius of most emission maps is thus set by the sensitivity limit of the telescope (see the companion paper of Ladd et al. 1991b for further discussion of observed emission maps and their boundaries).

6. DISCUSSION

6.1. *Summary of the Results*

In this paper, we have presented an asymptotic theory which can be used to interpret observed emission maps of protostellar objects. We have focused our discussion on the submillimeter portion of the spectrum where nearby protostellar objects can be spatially resolved. In this regime, we have obtained an asymptotic expansion for the specific intensity (see eq. [3.16]); this expansion shows the dependence of the radiation field I_ν on the basic physical structure of the protostellar envelope—the density and temperature distributions. We have also obtained an (independent) asymptotic expansion for the convolution of a specific intensity profile with a Gaussian response function of a telescope (see eq. [4.14]).

These results can be used to calculate directly observable quantities. For example, we have calculated the expected monochromatic luminosity profile for a power-law I_ν profile (see eq. [5.8] and [5.10]); by comparing these results to observations, an effective power-law index for the specific intensity is determined. This index m can then be compared to the expected power-law index μ of the specific intensity profile (see eq. [3.18]) and can thus constrain the physical properties of the protostellar envelope. We have also provided a more general treatment of the problem (see Appendix B) which remains valid when the specific intensity cannot be considered as a pure power law.

The asymptotic results of this paper depend on two large parameters. The first, λ_I, measures the degree to which the specific intensity integral (see eq. [3.2]) is peaked about the point of closest approach ($s = 0$). The second, λ_B, measures the degree to which the beam response function changes faster than the physical background. In the limit $\lambda_B \to \infty$, the observed flux density is probing a single line of sight—that corresponding to the direction of the beam center. In the limit $\lambda_I \to \infty$, the specific intensity integral is probing a single point along its line of sight—that corresponding to the point of closest approach of the ray to the center of the envelope. Thus, in the limit that both λ_B and λ_I are large, observations can probe a single point in the protostellar envelope. However, these limits are not realized in actual practice and the expansions presented in this paper provide the leading order corrections to this idealized limit.

The analytic results of this paper are meant to be complementary to numerical studies of this type. Numerical evaluation of the integrals (for I_ν and L_ν) will ultimately be of greater accuracy than the results obtained here. By obtaining analytic results, however, we have directly shown the dependence of the observational quantities on the underlying physical quantities of the problem. In this current study, the density and temperature distributions of the protostellar envelope were taken as given. In a self-consistent calculation, the density distribution is determined by the equations of motion for the collapse flow and the temperature distribution is determined by the condition of radiative balance. However, since these distributions have been calculated previously (see § 2 and the references therein), we can use the self-consistent values as input parameters for our formulae.

6.2. *Recipe for Interpretation of Observations*

In order to illustrate the possible uses of the asymptotic theory of this paper, we now present a step by step outline for interpreting observations of protostellar sources. The ideal range of wavelengths for this sort of procedure is 350 μm $\le \lambda \le$ 1100 μm. For shorter wavelengths, the approximations used to compute the monochromatic luminosity profile (in § 5) begin to break down (see Appendix B) and the sources are not expected to be well resolved; at longer wavelengths, the total emitted energy is too small to make emission maps with high signal-to-noise ratios. In using the following outline, keep in mind that individual cases will vary and that this recipe is meant to be suggestive rather than definitive.

1. Begin with observed emission maps of protostellar sources. For a given frequency of observation, produce a measured monochromatic luminosity profile $L_\nu(R)/L_\nu(0)$, i.e., obtain the relative flux density as a function of radius R from the center of the source. If the observations are of sufficiently high quality (high signal-to-noise ratio), each independent scan across the source can be considered as a separate flux profile; in practice, however, the observations might need to be circularly averaged to obtain a single flux profile with a reasonable signal-to-noise ratio.

2. Calculate the effective power-law index m for the observed flux profile. If only a single value of $L_\nu(R)$ is measurable (for $R > B$), simply use equation (5.8) to obtain the effective index m. If two independent values $L_\nu(R_1)$ and $L_\nu(R_2)$ are available (where both R_1, $R_2 > B$), use equation (5.10) to solve for both the index m and the relative contribution γ_ν of the central source. If additional measurements are available, find the overall best fit to the flux profile and thereby determine an effective power-law index $m_{\rm eff}$.

3. Repeat the above procedure for every frequency for which data exists. The result will be an effective index $m_{\rm eff}(\nu)$ which is a function of frequency.

4. Compare the observationally determined index $m_{\rm eff}$ with the theoretically expected index μ from equation (3.19). To leading order $m_{\rm eff} + 1 = \lambda_I = p + qQ$ [recall that $Q = Q(x)$, where $x = h\nu/kT$]. To specify the temperature, we must know both the coefficient $T_{\rm eff}$ and the power-law index q. We thus have three parameters (p, q, and $T_{\rm eff}$) and observations at three frequencies should suffice to estimate their values.

5. If more data are available (in addition to the minimal amount required to solve for p and q), the estimated values of p and q can be checked for self-consistency. (Notice that this procedure is quite similar to that used to calibrate data in the submillimeter continuum and should thus be both self-explanatory and highly familiar to seasoned submillimeter observers.) The result of this procedure should be "error bars" which estimate the uncertainty in assigning single power-law indices p and q to the density and temperature distributions respectively.

6. If the resulting values for p, q, and $T_{\rm eff}$ suggest that the approximations of § 5 are breaking down, better results can be obtained by using the more general treatment of the problem given in Appendix B. In this general treatment, the central beam integral must be done numerically and the integral is a function of all three variables p, q, and $T_{\rm eff}$. As a result, the conversion between the observed quantities $[L_\nu(R)/L_\nu(0)]$ and the physical variables involves a search of a three-dimensional parameter space.

7. If an absolute (calibrated) measurement of $L_\nu(R)$ is available, the leading coefficient of the monochromatic luminosity can also be determined (see eqs. [3.16] and [5.3]). This coefficient is proportional to $\kappa_\nu \rho_0$ in our parametric representation (see eq. [2.4]) and is proportional to $\kappa_\nu C$ in the protostellar theory.

6.3. *Future Work*

Although the results of this paper should be useful for interpreting existing and future observational data, further analysis of this kind can be performed. In this present work, we have only calculated the two leading order terms (in $1/\lambda_I$) of the specific intensity expansion; higher order corrections can be obtained as the observations become increasingly precise. In addition, further analytical work can be done to study protostellar emission in other regimes, e.g., in the near-infrared where the optical depth attenuation factor is large (and therefore *not* slowly varying as assumed here). If analytic approximations for the specific intensity I_ν can be obtained over the entire wavelength range of interest, these results can be used as a starting point for a self-consistent radiative transfer calculation. Although these calculations have already been performed for the case of spherical symmetry, calculations in higher dimensions (e.g., axial symmetry) remain difficult because of the large number of required computations (see however, Dent 1988 and Efstathiou & Rowan-Robinson 1990 for preliminary calculations in two spatial dimensions); analytic approximations may be useful in this context.

On the observational side, the results of this paper suggest a somewhat different observing strategy than is normally used. In an ideal case, observations should be performed over the wavelength range 350 μm $\le \lambda \le$ 1100 μm. Observations at shorter wavelengths ($\sim$100 μm) are invaluable for defining the peaks of the spectral energy distributions (e.g., Ladd et al. 1991a), but are not as useful for determining the spatial structure of protostellar sources. The most important observed quantity for determining spatial structure is the *relative* monochromatic luminosity profile $L_\nu(R)/L_\nu(0)$ and the goal of observational work is thus to obtain these profiles with the highest possible signal to noise ratios. To achieve this goal, relatively more observing time should be spent on determining $L_\nu(R)$ for large R and relatively less time should be spent on obtaining absolute calibrations. Notice also that a complete emission map with low signal to noise is not as useful as a single scan across the sources (a single flux profile) with higher signal to noise. Finally, notice that the 600 μm band, which is notoriously difficult to calibrate, can be profitably employed in this context because only a relative calibration is required.

I would like to thank Gary Fuller, Ned Ladd, Phil Myers, Phil Pinto, George Rybicki, Frank Shu, and Steve Stahler for stimulating discussions and useful comments. I would also like to thank an anonymous referee for useful comments regarding the presentation of this paper. This work was supported by a Center for Astrophysics Fellowship.

APPENDIX A

THE TEMPERATURE DISTRIBUTION

In this Appendix we derive an anlytic form for the temperature distribution of a protostellar envelope (see also Larson 1969; Adams & Shu 1985, 1986). This derivation is valid in the outer portion of the envelope where emission is optically thin (this portion of the envelope also corresponds to the size scales of interest for this paper). If we assume that all of the direct radiation from the central star/disk system is attenuated, the condition of radiative balance for the dust grains becomes

$$\int_0^\infty d\nu\, \kappa_\nu B_\nu[T] = \int_0^\infty d\nu\, \kappa_\nu \int \frac{d\Omega}{4\pi} I_\nu \quad \text{or} \quad \kappa_P a T^4 = \kappa_E \mathscr{E} , \tag{A1}$$

where we have introduced the frequency-averaged energy density $\mathscr{E}$ of the radiation field, the Planck mean opacity $\kappa_P(T)$, and the energy weighted mean opacity κ_E (a is the usual radiation constant). In the limit that the emission becomes optically thin, the distribution of the specific intensity in frequency does not change with radius and hence $\kappa_E \to$ *constant*. In this limit $\mathscr{E} = \mathscr{F}/c$, where $\mathscr{F}$ is the frequency integrated flux, which takes the simple form

$$\mathscr{F} = \frac{L}{4\pi r^2} , \tag{A2}$$

where L is the total luminosity of the protostar. We thus obtain the following relation for the temperature distribution

$$\kappa_P(T) T^4 = \frac{\kappa_E L}{4\pi a c} r^{-2} , \tag{A3}$$

where the right-hand side of the equation is independent of temperature. At low frequencies, the dust opacity κ_ν is expected to have a power-law form with an index β (see eq. [2.12]). For the relatively low temperatures of interest, we can therefore estimate the Planck mean opacity using equation (2.12) for κ_ν:

$$\kappa_P(T) = A\left(\frac{kT}{h}\right)^\beta \frac{\Gamma(4+\beta)\zeta(4+\beta)}{\Gamma(4)\zeta(4)} , \tag{A4}$$

where ζ is the Riemann zeta-function and Γ is the gamma function (see, e.g., Abramowitz & Stegun 1965). Combining all of the above results, we thus obtain the radial dependence of the temperature distribution

$$T(r) = \left[\frac{\kappa_E L}{4\pi a c}\left(\frac{h}{k}\right)^\beta \frac{\Gamma(4)\zeta(4)}{A\Gamma(4+\beta)\zeta(4+\beta)}\right]^{1/(4+\beta)} r^{-2/(4+\beta)} , \tag{A5}$$

which should be valid over most of the range in size scales probed by the observations. Notice that we have assigned a single temperature distribution to the dust grains even though the dust grains have different compositions and sizes. Calculations which include multiple temperature distributions (for multiple components) suggest that this assumption is basically valid (see Wolfire & Cassinelli 1986, 1987).

APPENDIX B

GENERAL TREATMENT OF THE CENTRAL BEAM INTEGRAL

In this Appendix, we present a more general form of the monochromatic luminosity profile (see eqs. [5.8] and [5.10]). The derivation given in the text breaks down at "short" wavelengths ($\lambda < 350\ \mu$m) because the power-law form for the specific intensity profile becomes invalid. The treatment given in this Appendix remains valid over the entire range of submillimeter wavelengths (100 μm $\leq \lambda \leq$ 1100 μm). On the other hand, this generalization cannot be done completely analytically and the results are not as "clean" as those of § 5 in the text.

The expansion of equation (5.3) for the quantity $\mathscr{L}_\nu(R)$ remains valid for essentially all cases of interest. However, we need to recalculate the central beam integral for $\mathscr{L}_\nu(0)$. It is convenient to write the specific intensity I_ν in terms of its value at R:

$$\varpi I_\nu(\varpi) = R I_\nu(R)\left(\frac{\varpi}{R}\right)^\alpha \frac{e^{x_R} - 1}{e^x - 1} , \tag{B1}$$

where $x = h\nu/kT$ (as usual), $x_R \equiv x(R)$, and where the index α is given by our asymptotic expansion of § 3, i.e.,

$$\alpha = 2 - p - \frac{q}{2} P + \dots , \tag{B2}$$

where we have neglected higher order terms. The monochromatic luminosity in the central beam can then be written in the form

$$\mathscr{L}_\nu(0) = 8\pi^2 \mathscr{N} I_\nu(R) R^2 \int_0^\infty dv\, v^\alpha \frac{e^{x_R} - 1}{e^x - 1} \exp\left[-v^2 \lambda_B/2\right] , \tag{B3}$$

where we have written the variable of integration as $v = \varpi/R$ [notice that $x = x(v) = x_R v^q$]. When the central source contribution can be neglected (i.e., when $\mathscr{L}_\nu = L_\nu$), the generalized monochromatic luminosity profile can be written

$$\frac{L_\nu(R)}{L_\nu(0)} = \frac{1}{\lambda_B} \frac{1}{K(p, q, x_R, \lambda_B)} \left[1 + \frac{m^2}{2\lambda_B} + \frac{m^2(m+2)^2}{8\lambda_B^2} + \mathscr{O}\left(\frac{1}{\lambda_B^3}\right)\right] , \tag{B4}$$

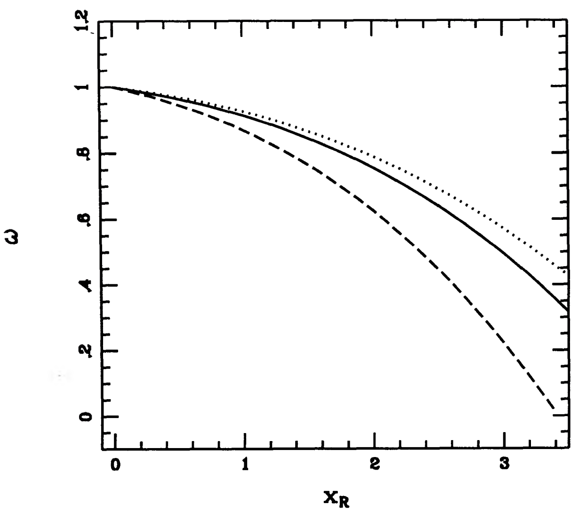

FIG. 4.—Relative error in the central beam integral as a function of x_R. The quantity ω is the ratio of the monochromatic luminosity at $R = B$ given by the power-law approximation of § 5 to that given by the numerical treatment of Appendix B. The various curves correspond to $p = 3/2$ and $q = 1/3$ (*solid line*); $p = 1$ and $q = 2/5$ (*dotted line*); $p = 3/2$ and $q = 2/5$ (*dashed line*).

where we have defined the function K through

$$K(p, q, x_R, \lambda_B) = \int_0^\infty dv\, v^\alpha \frac{e^{x_R} - 1}{e^x - 1} \exp\left[-v^2 \lambda_B/2\right] . \tag{B5}$$

Since λ_B is a known quantity for a given observation, the function K contains three free parameters which can be taken to be p, q, and some effective temperature T_{eff}. Notice also that, in general, the integral for K must be performed numerically. Equations (B4) and (B5) provide a generalized version of equation (5.8) in the text. The corresponding generalization for the case of nonvanishing central source flux (see eq. [5.10]) can be found similarly.

The approximations of § 5 can now be quantified. Let us define ω to be the ratio of the monochromatic luminosity profile given by § 5 (see eq. [5.8]) to that given by the treatment of this appendix (see eq. [B4]). If we specify $R = B$ and the power-law indices p and q of the density and temperature distributions, the ratio ω is a function of x_R only. Figure 4 shows ω as a function of x_R for a few representative values of the indices p and q. The deviation of ω from unity determines the validity of the power-law approximation of § 5.

REFERENCES

Abramowitz, M., & Stegun, I. A. 1965, Handbook of Mathematical Functions (New York: Dover)
Adams, F. C. 1990, ApJ, 363, 578
Adams, F. C., Lada, C. J., & Shu, F. H. 1987, ApJ, 312, 788
Adams, F. C., & Shu, F. H. 1985, ApJ, 296, 655
———. 1986, ApJ, 308, 836
Beichman, C. A. 1987, ARA&A, 25, 521
Beichman, C. A., Myers, P. C., Emerson, J. P., Harris, S., Mathieu, R. D., Benson, P. J., & Jennings, R. E. 1986, ApJ, 307, 337
Bleistein, N., & Handelsman, R. A. 1986, Asymptotic Expansions of Integrals (New York: Dover)
Butner, H. M., Evans, N. J., Lester, D. F., Levreault, R. M., & Strom, S. E. 1991, ApJ, in press
de Bruijn, N. G., 1981, Asymptotic Methods in Analysis (New York: Dover)
Dent, W. R. F. 1988, ApJ, 325, 252
Draine, B. T., & Lee, H. M. 1984, ApJ, 285, 89
Efstathiou, A., & Rowan-Robinson, M. 1990, MNRAS, 245, 275
Erdelyi, A. 1956, Asymptotic Expansions (New York: Dover)
Hildebrand, R. H. 1983, QJRAS, 24, 267
Keto, E. R. 1989, preprint
Ladd, E. F., Adams, F. C., Casey, S., Davidson, J. A., Fuller, G. A., Harper, D. A., Myers, P. C., & Padman, R. 1991a, ApJ, 366, 203
———. 1991b, ApJ, 382, 555
Larson, R. B. 1969, MNRAS, 145, 297
Myers, P. C., Fuller, G. A., Mathieu, R. D., Beichman, C. A., Benson, P. J., Schild, R. D., & Emerson, J. P. 1987, ApJ, 319, 340
Shu, F. H. 1977, ApJ, 214, 488
Shu, F. H., Adams, F. C., & Lizano, S. 1987, ARA&A, 25, 23
Stahler, S. W., Shu, F. H., & Taam, R. E. 1980, ApJ, 241, 637
Terebey, S., Shu, F. H., & Cassen, P. 1984, ApJ, 286, 529
Walker, C. K., Adams, F. C., & Lada, C. J. 1990, ApJ, 349, 515
Wolfire, M. G., & Cassinelli, J. P. 1986, ApJ, 310, 207
———. 1987, ApJ, 319, 850
Wynn-Williams, C. G. 1982, ARA&A, 20, 587
Yamashita, T., Sato, S., Kaifu, N., & Hayashi, S. S. 1990, ApJ, 365, 615
Yorke, H. W., & Shustov, B. M. 1981, A&A, 98, 125